Degenerate four-wave mixing in a resonant homogeneously broadened system

D. G. Steel, R. C. Lind, and J. F. Lam
Hughes Research Laboratories, 3011 Malibu Canyon Road, Malibu, California 90265
(Received 19 February 1980; revised manuscript received 29 December 1980)

Detailed measurements have been made of degenerate four-wave mixing (DFWM) in a resonant homogeneously broadened gas. The measurements were performed in SF_6 using a pulsed CO_2 laser operated on the 10.4-μm branch. A pulse width of 1.2 nsec was used to reduce effects of collisional relaxation. Data are also presented for pulse widths of 140 nsec. At high-energy fluences ($\sim$0.1 J/cm^2) pulse breakup is observed and is believed to arise from multiple-photon effects. The data obtained with the short pulse width are compared to a four-level saturable-absorber model where excellent agreement is obtained when pump absorption is included. The qualitative behavior of DFWM due to dispersion is also demonstrated in the wings of the SF_6 absorption spectrum. Peak reflectivities of 38% were readily obtained. In addition contributions due to a coherent three-level nonlinearity are presented showing a contribution equal to the measured saturable contribution.

INTRODUCTION

Degenerate four-wave mixing (DFWM) is a third-nonlinear optical process being studied by our group and others for application to basic studies of atomic and solid-state systems (e.g., high-resolution spectroscopy and carrier diffusion rates) as well as optical phase conjugation (wavefront reversal) in real imaging or focusing systems. The latter permits correction of optical systems when performance is limited by aberrations and dispersion.

The high-resolution-spectroscopy capability of DFWM was first experimentally recognized by Liao and colleagues in sodium.[1] Using a tunable narrow band cw dye laser they measured sub-Doppler line shapes on the $3s\,^2S_{1/2} - 3p\,^2P_{3/2}$ one-photon transition in sodium. Lam *et al.* have shown that using the same transition in sodium they were able to isolate the Zeeman coherence using DFWM.[2] Additional measurements are under way by both groups to study collision effects and excited state nonlinearities, respectively. Using a pulsed dye laser, Liao showed that DFWM could also be used to perform Doppler-free measurements of the collisionally induced transverse relaxation rate on the two-photon transition $3s$-$4d$ in sodium.[3] This technique was used by Steel and Lam[4] to measure the collisionless dephasing rate in SF_6. The theoretical description for DFWM including motion has been given by Wandzura[5] for one-photon processes and by Lam[6] and Sargent[7] for two-photon processes showing the Doppler-free property. The use of DFWM for high-resolution spectroscopy has recently attained increased importance because it has been demonstrated that near shot-noise limited detection may be achieved using heterodyne detectors.[8]

DFWM was first proposed by Stepanov[9] for phase conjugation using a real time holographic description. Since the inception of off-axis holography, it has been realized that if the reconstruction beam is conjugate to the reference beam, a "pseudo" image is produced that is phase conjugate (wavefront reversed) to the original image produced by the scene beam.

A review of DFWM and phase conjugation in third-order nonlinear materials is given by Yariv.[10] The phase-conjugate and nonlinear properties have been investigated in many groups with gain in the signal eventually being observed in CS_2 (Ref. 11) and Si (Ref. 12). In contrast to these materials, Abrams and Lind[13] have shown theoretically that two-level resonant absorbers can provide a medium capable of yielding gain at much lower intensities. Many resonant systems including rubidium,[14] sodium,[15,1,16] CO_2 (Ref. 17), and SF_6 (Ref. 18) have been shown to manifest the expected nonlinear response with gains in excess of 100 observed in sodium. The pulsed experiments in sodium and rubidium were performed in the adiabatic following limit.

This paper presents experiments and comparison with theory of DFWM using SF_6 as the resonant saturable absorber and a pulsed CO_2 laser. In an earlier paper, we presented preliminary parametric data and results demonstrating phase conjugation in the presence of severe aberrations. The present work presents an experimental study in both the long-pulse ($\tau_p \gtrsim T_r$) and short-pulse ($\tau_p < T_r$) regime where T_r is a characteristic relaxation time in SF_6. For the short-pulse limit excellent agreement is obtained with an improved version of existing two-level theory. A four-level model similar to Brunet[19] was assumed and pump absorption was included in a phenomenological way. Effects of motion can be ignored[5] in the short-pulse limit but are important for longer pulses.[20] In addition we present data obtained using a two-photon resonance that also provides returns comparable to the usual one-photon process. The two-photon process is often referred to

as a coherent process (in the atomic sense involving T_2^{-1} relaxation rates) where as the one-photon process is incoherent since the latter effect involves population effects (T_1^{-1} relaxation rates). Detailed understanding of the various physics contributing to DFWM in resonant systems has been demonstrated to be critically important to the design and interpretation of high-resolution spectroscopy experiments.

Detailed measurements and comparison with theory has also been made for cw DFWM in SF_6 under inhomogeneous broadening conditions. Large returns ($R \sim 0.2\%$) has been obtained along with relatively high spectral resolution ($\Delta\nu \sim 5$ MHz). This work is to be published separately.[21]

REVIEW OF THEORETICAL MODEL FOR RESONANT DFWM

In general, the analysis proceeds based on the third-order nonlinear response of an isotropic medium. The general configuration is shown in Fig. 1. Two pump beams ($\vec{E}_f$ and $\vec{E}_b$) are incident on the medium and are in general (though not necessarily) counter propagating. It is assumed that the pumps are aberration-free plane waves. The proble ($\vec{E}_p$) is then incident at some angle θ with respect to the forward pump (E_f). The signal ($\vec{E}_s$) is produced by the nonlinear polarization, which in general is given by

$$\vec{p}^{NL} = 3\chi^{(3)}(\vec{E}\cdot\vec{E})\vec{E}, \tag{1}$$

where

$$\vec{E} = \tfrac{1}{2}\sum_i \vec{E}_i(r_i)e^{i(\omega t - \vec{k}_i\cdot\vec{r})} + \text{c.c.}; \tag{2}$$

3 is the degeneracy factor, and i is summed over forward, backward, probe, and signal.

For DFWM, the phase-matching conditions are given by

$$\omega_f + \omega_b - \omega_p - \omega_s = 0,$$
$$\vec{k}_f + \vec{k}_b - \vec{k}_p - \vec{k}_s = 0. \tag{3}$$

The polarization for the signal wave can then be written as

$$\vec{p}_s^{NL}(\omega_s = \omega_f + \omega_b - \omega_p) = \tfrac{3}{2}\chi_b^{(3)}(\vec{E}_f\cdot\vec{E}_p^*)\vec{E}_b + \tfrac{3}{2}\chi_f^{(3)}(\vec{E}_b\cdot\vec{E}_p^*)\vec{E}_f + \tfrac{3}{2}\chi_p^{(3)}(\vec{E}_b\cdot\vec{E}_f)\vec{E}_p^* + \text{c.c.} \tag{4}$$

A similar expression for $\vec{P}_p^{NL}$ is found with $E_p \leftrightarrow E_s$.

One then proceeds to solve the coupled Maxwell wave equations between the signal and the probe. The details of this general calculation can be found elsewhere.[22] Physically, the first two terms usually represent an interaction between the probe and one of the pumps producing a spatial modulation of the index which results in a scattering of the remaining pump. The third term generally represents a coherent term. It can result from a two-photon resonance with a scaler susceptibility oscillating at 2ω, $(\vec{E}_b\cdot\vec{E}_f)$. However, it can also result from a coherent coupling between the probe and a pump producing a tensor susceptibility, $(\vec{E}_b\vec{E}_p^*)$ or $(\vec{E}_f\vec{E}_p^*)$.

Although in typical $\chi^{(3)}$ materials the nonlinearity produces purely refractive changes, in resonant saturable absorbers both nonlinear refractive and absorptive changes can occur via incoherent and coherent atomic interactions. In materials with large absorption and low saturation intensities, these effects can be quite large compared with those more common nonlinear materials such as CS_2 and Ge.

In the absence of pump absorption or depletion and no motion a rigorous derivation of the nonlinear response of a two-level saturable absorber may be made[13] by assuming a homogeneously broadened saturating two-level system described by the susceptibility $\chi(E)$:

$$\chi(E) = -\frac{2\alpha_0}{k}\frac{(i+\delta)}{(1+\delta^2+|E/E_s|^2)}, \tag{5}$$

where $\delta = (\omega - \omega_0)T_2$ is the normalized laser detuning from line center, $|E_s|^2 = \hbar^2/T_1T_2\mu^2$ is the line center-field saturation parameter, $\alpha_0 = \mu^2\Delta N_0 T_2 k/2\epsilon_0\hbar$ is the line center small signal *field* attenuation coefficient, $k = \omega/c$, and $T_1(T_2)$ is the longitudinal (transverse) relaxation rate. Assuming $E = E_0 + \Delta E$, where $E_0 = E_f + E_b$ and $\Delta E = E_p + E_s$ and ignoring pump absorption, the polarization is expanded about E_0 assuming $\Delta E/E_0 \ll 1$. Using this expansion of the fields given in Eq. (2), the coupled equations of interest are

$$\frac{dE_s}{dz} = \alpha E_s + iK^*E_p^*,$$
$$\frac{dE_p}{dz} = -\alpha^*E_p + iKE_s, \tag{6}$$

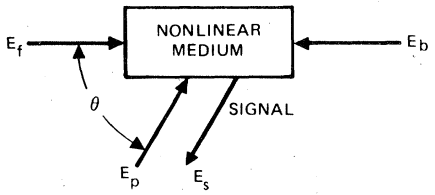

FIG. 1. Geometry for DFWM. In general, the pump beams (E_f and E_b) are counter propagating. In this case the signal (E_s) produced by the nonlinear response is counter propagating to the probe (E_p).

where

$$\alpha = \frac{\alpha_0}{n}\frac{1}{1+\delta^2}\frac{1+2I/I_s'}{(1+4I/I_s')^{3/2}}, \tag{7}$$

$$K^* = i\frac{\alpha_0}{n}\frac{1-i\delta}{1+\delta^2}\frac{2I/I_s'}{(1+4I/I_s')^{3/2}} \tag{8}$$

and $I_s' = I_s(1+\delta^2)$ is the frequency-dependent saturation intensity and n is the index of refraction including the nonlinear anomalous dispersion. In this case the reflection coefficient (the ratio of signal intensity to probe intensity) is given by

$$R = \frac{|K\sin wL|^2}{|w\cos wL + \alpha\sin wL|^2}, \tag{9}$$

where

$$w = (|K|^2 - \alpha^2)^{1/2}. \tag{10}$$

A plot of the reflectivity for various parameters is shown in Fig. 2. Several interesting properties can be seen by studying the figure. In an absorbing medium when $\delta = 0$ (i.e., line-center operation), the dispersive contribution is zero resulting in a purely absorptive interaction. However, if the laser is detuned, the dispersive contribution begins to dominate the absorptive contribution for $I/I_s \gg 1$. The absorption becomes negligible and the reflectivity can easily exceed that obtained on line-center operation with gain readily obtained ($R > 1$). For completeness, curves are also shown in Fig. 2 for an inverted two-level system, characterized by a $g_0 l$ (where g_0 is the electric field gain per unit length). In general, the two-level system has a resonance condition established by

$$\tan wL = w/\alpha, \tag{11}$$

which manifests itself as a singularity. The singularity is eliminated if the system is treated by a fully nonlinear theory to allow for

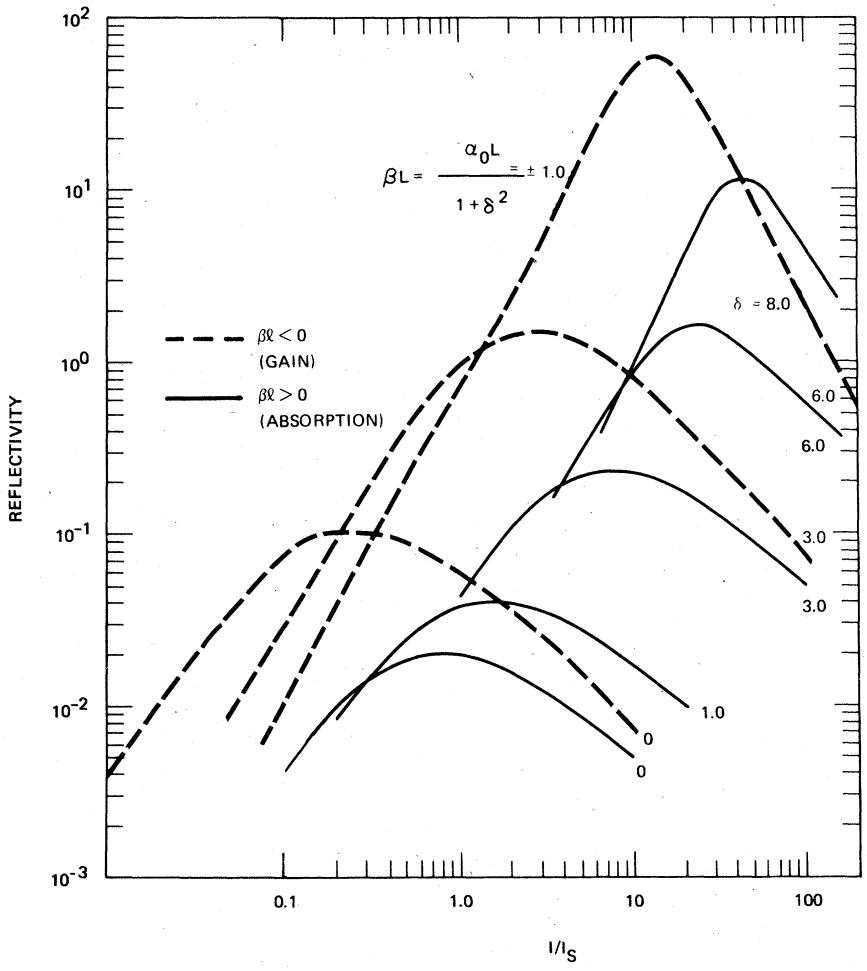

FIG. 2. Reflectivity as a function of the normalized laser intensity. Curves on the right (solid line) are for absorptive two-level systems and curves on the left (dotted line) are for an inverted two-level system.

pump depletion.

The above discussion pertains to the first two terms of the polarization given in Eq. (4). The third term, called the coherent interaction term, can be generated by various interactions in a resonant system. Of particular interest is the contribution in a three-level system described by a two-photon resonance. The description assumes three levels with levels 1 and 2, and 2 and 3 connected by dipole-allowed transitions. The preliminary description of this interaction has been given by Liao, Economou, and Freeman,[3] and Steel and Lam.[4] A detailed description of two-photon DFWM is given by Lam[6] and Sargent.[7] This term can best be understood by considering the simultaneous interaction of the forward and backward pumps producing a two-photon coherent excitation between states $|1>$ and $|3>$ oscillating at a frequency 2ω (twice the laser frequency). The interaction of the two-photon coherence with a third field (E_p) via an induced electric dipole coupling leads to the generation of the signal wave oscillating at the laser frequency. The phase-matching conditions are the same as in Eq. (3) insuring that the signal will be counterpropagating to the probe for counterpropagating pumps.

Assuming a three-level model shown in Fig. 3, a perturbation solution may be derived from the density matrix equations. Then using the polarization expression $\vec{P} = \mathrm{Tr}\,\vec{\mu}\rho$ we find[4]

$$\vec{P} = -\frac{N_0}{4ih^3}\frac{|\mu_{12}|^2|\mu_{23}|^2(\vec{E}f\cdot\vec{E}b)\vec{E}_p^*}{[\gamma_{13}-i(\omega_{31}-2\omega)]}\frac{e^{i\vec{k}_p\cdot\vec{r}-i(\omega_{31}-\omega)t}}{(\gamma_{12}-i\Delta_{21})} \times\left(\frac{1}{(\gamma_{12}-i\Delta_{21})}+\frac{1}{(\gamma_{32}+i\Delta_{21})}\right), \tag{12}$$

where $\Delta_{21}=\omega_{21}-\omega\gamma_{ij}=\frac{1}{2}(\gamma_i+\gamma_j)$ and γ_i is the decay rate from level i. We note first that such a polarization is not characterized by a spatial modulation of the medium. Rather the nonlinear susceptibility is seen to oscillate in time at 2ω on resonance. We see that if the intermediate state is detuned greater than the intermediate linewidth, then the overall linewidth is given by γ_{13}. In this case the polarization may be written as

$$\vec{P} = +\frac{N_0}{4ih^3}\frac{\gamma_{13}+i(\omega_{31}-2\omega)}{\gamma_{13}^2+(\omega_{31}-2\omega)^2}\frac{|\vec{\mu}_{12}|^2|\vec{\mu}_{23}|^2}{\Delta_{21}^2} \times\vec{E}_f\cdot\vec{E}_b\vec{E}_p^*\,e^{i\vec{k}_p\cdot\vec{r}-(\omega_{31}-\omega)t}\,. \tag{13}$$

We note that as in the simple two-level model, this nonlinearity is characterized by an absorptive and dispersive component. Hence an expression for the reflectivity similar to Eq. (9) can be simply derived. As we note below, we shall observe that under certain conditions this polarization may give rise to signals as large as the usual two-level response. The more general description including the ac Stark shifts and saturation is given by Lam.[6]

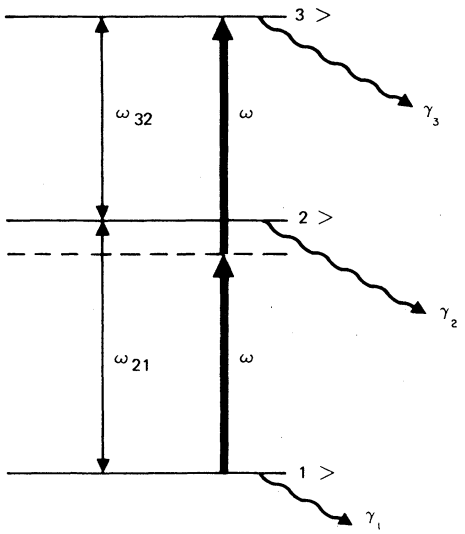

FIG. 3. Level diagram for a three-level system. The laser is at frequency ω while the level energies are at $\hbar\omega_{21}$ and $\hbar\omega_{32}$.

An additional interaction that can give rise to this third term is the tensor polarization (e.g., $\vec{E}_f\vec{E}_p{:}\vec{E}_b$) generated by Zeeman coherence from an induced electric quadrupole in degenerate resonant systems.[2] This is to be discussed in detail elsewhere[21] but as we mention below does not appear to be a significant interaction in SF_6 in our high pressure regime.

DFWM IN A FOUR-LEVEL SYSTEM

The idealized two- and three-level systems described above demonstrate very clearly the physical behavior of DFWM in a saturable resonant absorber. However, most atomic and molecular systems studied in the laboratory are usually complicated by the presence of other energy levels coupling to the optical interaction either directly through a dipole moment or indirectly through collisions. This is precisely the situation in SF_6 under our experimental conditions. In particular Brunet,[19] Garside,[23] and Armstrong[24] have shown that under certain conditions, SF_6 may be modeled as a four-level system. Figure 4 shows a typical level configuration assumed for SF_6. The population in the $\nu_6=1$ level is one half the ground-state population allowing for hot band transitions out of $\nu_6=1$. The ground state to $\nu_6=1$ transition is not IR active but the ν_3 mode is IR active. The cross sections σ_{34} and σ_{21} are in the ratio[23] of $\sigma_{34}/\sigma_{21}=1.5$. Hence, assuming comparable relaxation rates (implying comparable saturation intensities) we expect a nonlinear response from both trans-

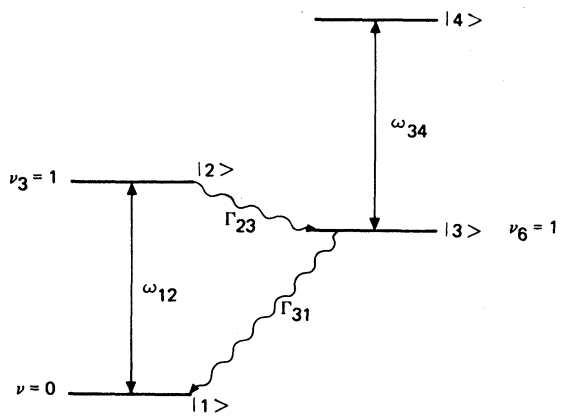

FIG. 4. Level diagram for a four-level system describing SF_6. Γ_{23} represents V-V relaxation between levels 2 and 3 and Γ_{31} represents the V-T relaxation from $\nu_6 = 1$ to the ground state.

itions. Owing to the large number of transitions actually available out of each level, the detuning can be assumed small, i.e., $\omega_{12} \simeq \omega_{34}$. For very short pulses, the collisional relaxation from $|2>$ to $|3>$ can be ignored ($\Gamma_{23} \sim \mu\text{sec}^{-1}\,\text{Torr}^{-1}$) but for longer pulses this rate along with Γ_{31} must be considered[19] since (in the cw limit) the laser will cause a net transfer of population from $|1>$ to $|3>$.

The modeling of DFWM for such a system including Γ_{23} and Γ_{13} due to collisions with arbitrary ω_{12} and ω_{34} has been developed by Lam.[25] However, if we assume $\tau_p < \Gamma_{23}^{-1}$ and Γ_{13}^{-1} then we can derive all the relevant behavior by a slight modification of the above DFWM model. We find the reflectivity is still given by Eq. (9) but K, α, and ω are redefined for the decoupled four-level system. In this case we can write α and K as $\alpha = \alpha_{12} + \alpha_{34}$ and $K = K_{12} + K_{34}$, where

$$\alpha_{ij} = \alpha_{ij}^0 \frac{1}{1+\delta_{ij}^2} \frac{1 + 2I/I_{ij}^s}{(1 + 4I/I_{ij}^s)^{3/2}}, \tag{14}$$

$$K_{ij}^* = i\alpha_{ij}^0 \frac{1 - i\delta_{ij}}{1+\delta_{ij}^2} \frac{2I/I_{ij}^s}{(1 + 4I^s/I_{ij}^s)^{3/2}}$$

$$\equiv iA_{ij}(1 - \delta_{ij}), \tag{15}$$

$$I_{ij}^{s'} = I_{ij}^s(1 + \delta_{ij}^2), \tag{16}$$

and δ_{ij} is the normalized detuning for the ij transition. The definition of w remains unchanged; i.e., $w = (|k|^2 - \alpha_R^2)^{1/2}$ and the reflectivity is given by Eq. (9): $R = |k \sin wL|^2 / |w \cos wL + \alpha_R \sin wL|^2$. The interesting term is $|k|^2$. We can write this as

$$|K|^2 = A_{12}^2(1 + \delta_{12}^2) + A_{34}^2(1 + \delta_{34}^2) + 2A_{12}A_{34}(1 + \delta_{12}\delta_{34}). \tag{17}$$

The first two terms represent the sum of the individual responses while the third term represents an interference effect. If δ_{12} and δ_{34} are opposite in sign we observe a destructive effect thus reducing the reflectivity. Physically the effect of this four-level model is to produce substantially different macroscopic behavior than anticipated by Fig. 2. The interference terms can actually produce a significant minima as a function of I in the reflectivity. As we see below, if $I_{12}^{s'} < I_{34}^{s'}$ and $\alpha_{12} < \alpha_{34}$, a double maxima in the reflectivity is produced when pump absorption is included. The details of this model including finite Γ_{23} and Γ_{13} are discussed separately. However, we have found that this model coupled with a phenomenological pump absorption gives excellent agreement with our experiments.

EXPERIMENTAL CONFIGURATION

The basic configuration for the CO_2 laser is shown in Fig. 5. The oscillator was comprised of a high-pressure Tachisto TEA discharge and a low-pressure continuous cs discharge to ensure single longitudinal mode operation. Two apertures were inserted in the oscillator cavity to assure TEM_{00} operation. The laser was grating tuned as shown and stabilized by piezoelectrically controlling the cavity length. The basic oscillator provided a gain switched pulse (no tail) with a controlled width of 140 to 200 nsec. For short-pulse experiments, a 1-nsec pulse could be extracted from the main pulse using an electrooptic switch from II-VI, Inc. The oscillator output was amplified using a Lumonics 101 TEA discharge configured for three passes using lenses to image the input through the amplifier which included a spatial filer. The beam then freely propagated to the experimental area.

The arrangement for our experimental studies of DFWM is shown in Fig. 6. We chose this arrangement for the counter propagating pumps since the more common approach of retroreflecting the forward pump to produce the backward pump leads to complications in interpretation if there is significant absorption of the forward pump. We have observed important differences for pumps differing in intensity by only several percent. This problem usually only results for DFWM in saturable absorbers due to absorption of the forward pump. The probe beam is generated by reflection from the back surface of the principal beam splitter (a wedge). For the 1-nsec experiments, an adjustable beam delay line was included to match the path lengths. The DFWM signal was detected by either a fast Société Anonyme de Télécommunications (SAT) HgCdTe detector (LN_2 cooled), a slow high-sensitivity Santa Barbara Research Center

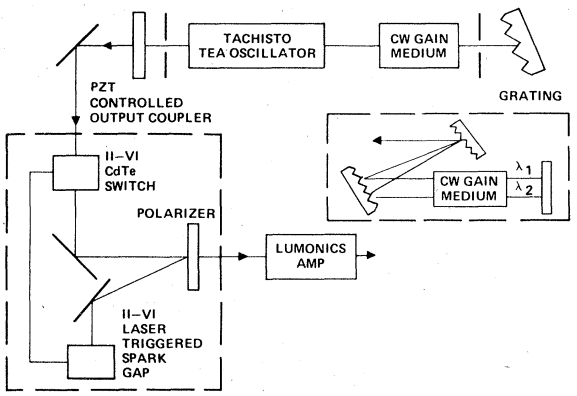

FIG. 5. Optical configuration for the laser used in DFWM. The laser could be operated in either a short-pulse or long-pulse mode, with either single-wavelength or multiwavelength capability.

(SBRC) HgCdTe detector (LN_2 cooled), or an infrared vidicon from ISI Corp. The input beam was monitored by a Rolfin photon drag detector. Polarization rotation was performed with CdS $\lambda/4$ of $\lambda/2$ wave plates. Polarization analyzers were of the wire grid variety.

The SF_6 was contained in an evacuated cell with NaCl windows. The cell was capable of maintaining a vacuum of 10^{-3} Torr when sealed off. We found, however, that it was necessary to evacuate the cell and refill with SF_6 every few minutes. Failure to do this resulted in a gradual increase in the nonlinear response. The effect was so dramatic as to eventually cause an order-of-magnitude increase in the signal at low laser intensities. We are presently unable to explain the cause of this effect. Reproducible results were finally obtained by evacuating the cell and refilling with SF_6 between each data point.

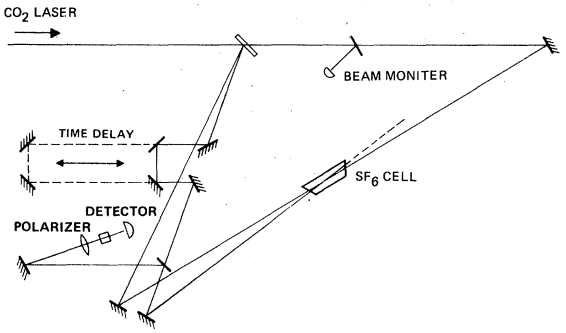

FIG. 6. Experimental configuration for measurements of DFWM in SF_6.

EXPERIMENTAL RESULTS AND COMPARISON WITH THEORY

The most important objective of these experiments was to quantitatively compare our experimental measurements of the nonlinear response arising from incoherent population dynamics to theoretical predictions of the four-level model. For these measurements, a 2-cm cell was used with a pump-to-probe angle of less than $\theta = 2°$ insuring sufficient overlap for 0.25 cm diameter beams. The pressure of SF_6 was 10 Torr, ensuring that SF_6 was homogeneously broadened by collisions. The laser was tuned to the P(20) line of the 10.4-μm branch and the pump intensities were carefully balanced. As mentioned above, a more general theory of resonant DFWM shows that if the pumps are unbalanced, the response is not as expected.[26] For these experiments, the ratio of probe intensity to pump intensity was kept constant and much less than one.

The experimental dependence of reflectivity on incident pump intensity was measured on the P(20) line for pulse widths of 1 and 140 nsec. Assuming a Γ_{23}^{-1} relaxation time of order 1 μsec Torr typical of V-V relaxation processes[27] we see at 10 Torr that V-V relaxation is important in the long-pulse experiments but negligible in the 1-nsec experiments. Hence, significantly different behavior is expected as observed in the results shown in Fig. 7.

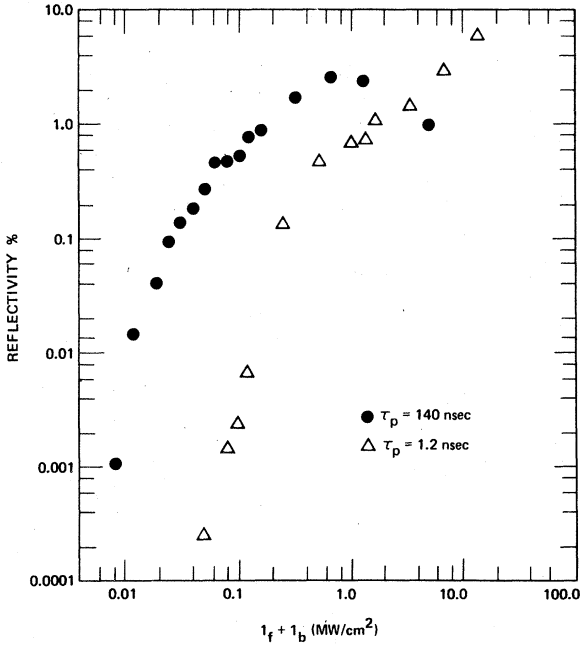

FIG. 7. Experimental measurement of reflectivity as a function of pump intensity. Data is shown for two different pulse widths.

One first observes that the curves while similar in shape are displaced from each other. Intuitively one expects this since the effective saturation intensity for the short-pulse experiments is much higher than for the quasi-cw long-pulse experiments. In general, $I_s = h\nu/\sigma T_1$, where T_1 is the longitudinal relaxation time. However, if $\tau_p < T_1$, we must redefine I_s as $I_s = h\nu/\sigma\tau_p$. Estimates of T_1 indicate reciprocal rates of order 100 nsec Torr. Hence we expect the 1-nsec data to be shifted to higher intensities by roughly an order of magnitude at 10 Torr. This behavior is confirmed by the data.

The point of inflection in both curves was anticipated in the above discussion based on an assumed four-level behavior. The lack of a dip in the reflectivity at that point implies that despite the presence of any anharmonic shift in the levels, the two transitions contributing to the DFWM signal are characterized by roughly the same frequency but different saturation intensities and absorption coefficients.

In the small-signal region of these curves we observe that the dependence on intensity is much stronger than the I^2 predicted by the original two-level model. This is caused directly by pump absorption which we discuss below in comparing with theory.

Finally, we observe the most dramatic difference between the two curves is that for $\tau_p = 140$ nsec the curve is decreasing rapidly at high intensities which no such effect observed for the $\tau_p = 1$ nsec data. Furthermore, comparison with two-level model predictions (Fig. 2) shows that the dependence on I on the high-intensity side of the peak is not as strong as observed in the data. We believe this sudden reduction in the nonlinear response is related to multiple-photon absorption and dissociation. The evidence of this arises from numerous reports in the literature of a fluence (ϕ) dependence for multiphoton absorption[28] corresponding to a threshold of $\phi \sim 0.1$ J/cm^2. Threshold is used loosely to denote the fluence where a significant fraction of molecules have been highly excited. This corresponds to an intensity threshold at this pulse width of order 700 kW/cm^2. One would expect a significant modification of the pulse width corresponding to the point when either the molecule was dissociated or was excited to a high lying state with corresponding reduction in α_0. This is shown in Fig. 8 where four pulse shapes are shown. Figure 8(a) shows the incident pulse shape as it comes from the laser. Figure 8(b) shows the actual signal pulse shape at low intensity ($I \sim 80$ kW/cm^2). The pulse shows clear narrowing as expected for a third-order nonlinear process. Figure 8(c) shows a broadened pulse at

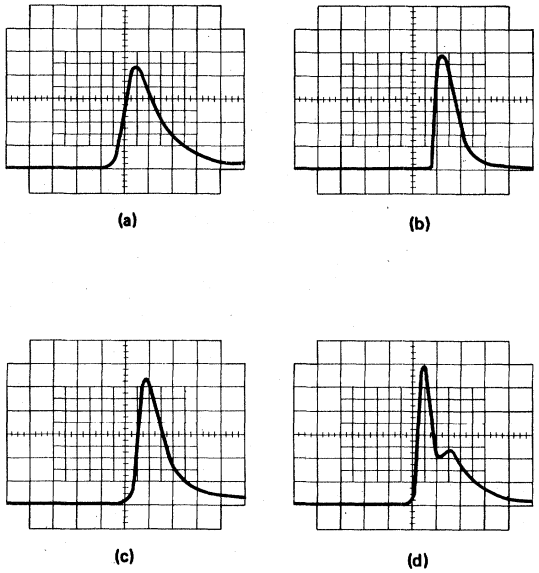

FIG. 8. The temporal response of the DFWM signal for various laser intensities (100 nsec/cm). (a) Laser reference pulse, (b) $I = 0.08$ MW/cm^2, (c) $I = 0.8$ MW/cm^2, (d) $I = 10$ MW/cm^2.

$I \sim 800$ kW/cm^2. The broadening is the result of a saturation of the nonlinearity. However, in Fig. 7(d) a complete breakup of the signal is observed believed to be caused by a multiphoton excitation of SF_6 to high lying states. Figure 8(d) was generated at $I = 10$ MW/cm^2 ($\phi \sim 1.4$ J/cm^2). The threshold for this temporal behavior corresponds to the intensity at the peak of the reflectivity curve for $\tau_p = 140$ nsec.

The data taken with $\tau_p = 1$ nsec shows no such behavior indicated above over the fluence range studied. Assuming the fluence threshold is pulse width independent, we can infer that such behavior would not be observed until we achieved a pump intensity of order 100 MW/cm^2.

The constraints of our modeling discussed above imply that an exact comparison can only be made for the data taken with $\tau_p = 1$ nsec. These constraints arise for three reasons. In the theory discussed above, the velocity term was assumed to be small. In particular, the general quantum mechanical transport equation can be written as

$$\left(\frac{\partial}{\partial t} + \vec{\mathbf{v}} \cdot \vec{\nabla}\right)\rho = \frac{1}{ih}[H, \rho] - \tfrac{1}{2}\{\Gamma, \rho\}, \tag{18}$$

where ρ is the density matrix, H is the Hamiltonian, and Γ is the decay matrix. The $\vec{\mathbf{v}} \cdot \vec{\nabla}$ operator represents the motion term. This term gives rise to the velocity broadening as well as velocity hole burning in inhomogeneously broadened media and thermal washout of spatial hole burning. It is the latter effect which impacts our experiments.

Spatial hole burning in homogeneously broadened gaseous laser material is well known because of the standing wave inside the laser cavity. The same effect occurs in DFWM in resonant gaseous saturable absorbers. Physically, spatial hole burning is caused by a spatial modulation of the population difference in a saturating resonant system. Such spatial modulation is produced by the interference of two waves with k vectors $\vec{k}_1$ and $\vec{k}_2$, respectively, and a corresponding fringe spacing of $\pi/k \sin\theta/2$ where θ is the angle between k_1 and k_2. The hole burning describes the spatially periodic saturated absorption and dispersion produced by interference of the two beams. In the steady state the magnitude of the population modulation would be determined by the ratio I/I_{SAT} if motion of the atoms or molecules was not a problem. However, including motion corrects for atoms which have been excited but drift into regions where atoms are not excited. Hence the modulation depth of the population difference is reduced by an amount determined by $\gamma^2 = (T_1 k V_0 \sin\theta/2)^{-2}$, where V_0 is the thermal velocity. For $\gamma \ll 1$ the transit time is short compared to the decay time causing thermal washout. For $\gamma \gg 1$ the thermal washout is negligible. In this case it implies the large angle grating is nearly completely washed out ($\gamma \sim 0.1$) while the small angle grating is only slightly reduced ($\gamma \sim 7$). For $\tau_p < T_1$, γ becomes $\gamma^2 \simeq [\tau_p V_0 \sin\theta/2\lambda]^{-2}$. For nsec-type pulses and the experimental conditions given, $\gamma \gg 1$ implying thermal motion is negligible for both gratings and hence, motion may be ignored.

The second two constraints on our modeling making it difficult to compare theory with the long-pulse experiments are collisional relaxation effects and multiple-photon absorption. While Lam has included V-V and V-T relaxation in the four-level model[25] of Fig. 4, we have chosen to ignore these complications in our modeling. This was necessary since the rates at 10 Torr are such that it is questionable as to whether a steady-state condition is really achieved in the gas for $\tau_p = 140$ nsec. However, for $\tau_p = 1$ nsec these effects may clearly be ignored. The additional complication of multiple-photon absorption mentioned above makes comparison at higher intensities unreasonable. Efforts to quantify this effect into a model for DFWM appear too difficult due to the current level of physical understanding of such processes.

For the above reasons the analysis and comparison with experiment was confined to the short-pulse experiments. Assuming the four-level model, we must evaluate the parameters which go into the theory. Itemizing them, they are $\alpha_{12}^0 L$, $\alpha_{34}^0 L$, δ_{12}, δ_{34}, and I_{34}^s/I_{12}^s. The independent variable can then be chosen to be I/I_{12}^s. Noting that the short-pulse small-signal (power) absorption coefficient[29] is given as 0.5 cm^{-1} $Torr^{-1}$, we can evaluate $\alpha_{12}^0 L$ and $\alpha_{34}^0 L$ using the cross-section ratio ($\alpha_{34}^0/\alpha_{12}^0 = 1.5$) and the thermal population distribution. Recall that α_{12}^0 and α_{34}^0 are the field absorption coefficients. For the interaction length of 2 cm at 10 Torr we find $\alpha_{12}L = 2.9$ and $\alpha_{34}L = 2.1$. It is also reasonable to assume that because of the six rotational transitions overlapping the P(20) line that $\delta_{12} \simeq 0$. Furthermore, a large density of states available for transitions out of the excited state (e.g., ν_6) would imply a similar assumption for $\delta_{34}(\delta_{34} \simeq 0)$.

Since very poor data is available on I_{12}^s and I_{34}^s we leave the ratio an adjustable parameter though it is known that $I_{34}^s/I_{12}^s > 1$. It would then be anticipated that while the $|1> \rightarrow |2>$ transition would saturate at I_{12}^s, the $|3> \rightarrow |4>$ transition would still contribute significant absorption, effecting not only the probe and signal amplitudes but also the pump amplitudes. While in the original modeling of two-level systems it seemed reasonable to ignore pump absorption in the region of peak reflectivity ($I \approx I_{SAT}$), this is clearly no longer justified in a four-level system. To account for this effect a phenomenological absorption model was used. In particular, we recall that the equations of motion for I_f and I_B are given by $dI_f/dx = -2\alpha_0 I_f/(1 + I_T/I_s)$ and $dI_b/dx = 2\alpha_0 I_B/(1 + I_T/I_s)$, where x is assumed positive in the direction of I_f and $I_T = I_f + I_b$. Ignoring standing wave effects one can easily show that the product $I_f I_b$ is a constant of the motion; i.e., $I_f(x) I_b(x) = \text{const}$. While the coupled equations can be simply integrated, the solution for $I_{f(b)}$ is implicit. However, an excellent approximation can be realized by setting $I_f I_b = I_f^0 I_b^0 e^{-2\alpha L}$, where the field absorption coefficient $\alpha = \alpha_{12} + \alpha_{34}$ and $\alpha_{ij} = \alpha_{ij}^0/(1 + I^0/I_{ij}^s)$ with the frequency dependence implicit to avoid confusion and the zero superscript on I refers to the boundary value. There is one additional correction needed. A more explicit form of Eqs. (7) and (8) show that in fact I is really $(I_f + I_b)/2$. Hence, approximation must be made. In this case it was assumed $I = I^0 e^{-2\alpha(L/2)}$. Despite the apparent simplicity of this model, comparisons of its predictions to an exact numerical model[30] have shown amazing agreement except in the limit of large $\alpha_0 L$ where the pump absorption correction fails. This is not totally without some explanation. The correction for saturating pump absorption becomes important only when $\alpha_0 L \gg 1$. However, in the original work studying the two-level model, it was shown that dependence of reflectivity on αl becomes very weak for $\alpha_0 L \gg 1$. But where the correction is most important is in the transition from the small

signal to large signal limit. Here, the model without pump absorption shows the reflectivity depends only quadratically on I while both the phenomenological correction and the numerical model show a much stronger dependence. Depending on the conditions this dependence may reach cubic arising from the decreased absorption in the pumps. This correction also shows that peak reflectivity occurs at a higher value of I/I_{SAT} than predicted by the model with no pump absorption. However, the peak valve of R is *not* significantly effected by this correction.

Using the value of I_{34}^s/I_{12}^s to achieve a best fit with the experimental data and assuming $\delta_{12} \sim \delta_{34} \sim 0$, the four-level model gave remarkable agreement with experiment as shown in Fig. 9. We see that the data corresponds to an I_{12}^s of order 0.2 MW/cm^2 in reasonable agreement with the published cross section and the expression for $I^s = h\nu/\sigma\tau_p$, where τ_p is the laser pulse width assuming $\tau_p \ll T_1$. As indicated above, the dependence of the reflectivity on pump intensity is stronger than quadratic due to pump absorption and is accurately given by the model. The inflection point in the reflectivity is seen to be a direct manifestation of four-level behavior. The ratio I_{34}^s/I_{12}^s was 55. This is somewhat arbitrary since it is determined by where the curve peaks which we were unable to study.

Hence, the four-level model has given excellent agreement with experiment using parameters consistent with those of SF_6. More detailed comparison with the model seems difficult due to the difficulty in incorporating the complex spectroscopy of SF_6. However, there are numerous qualitative properties which can be shown using SF_6.

In addition to saturation of the reflectivity for $I_{pump}/I_{sat} > 1$, we expect an additional saturation of reflectivity for $I_p/I_{sat} \simeq 1$ as I_p (the probe intensity) increases to approach the pump intensity. This saturation results from a reduction of the coupling coefficients as I_p contributes to saturating the absorption. The experimental behavior is shown in Fig. 10 for the P(20) line. Comparison with the model is not possible since the model is based on the assumption that $I_p/I_{pump} \ll 1$.

As indicated above due to the spectroscopy a detailed comparison of the effects of detuning appears difficult. Indeed, at the P(20) wavelength of CO_2 in the 10.4-μm branch, there are six Q branch transitions available to participate in the interaction in addition to hot band transitions.[31] Each branch has its own resonance detuned by some amount (of order 100 MHz) from the P(20) line. However, we were able to demonstrate qualitatively the increase in signal when detuned. The reflectivity was measured for various laser lines extending over the entire range of the SF_6 absorption spectrum. Each measurement was optimized as a function of pressure for that frequency. The results are shown in Fig. 11, which also shows the total SF_6 absorption spectrum taken from Brunnet.[22] In the center of the absorption

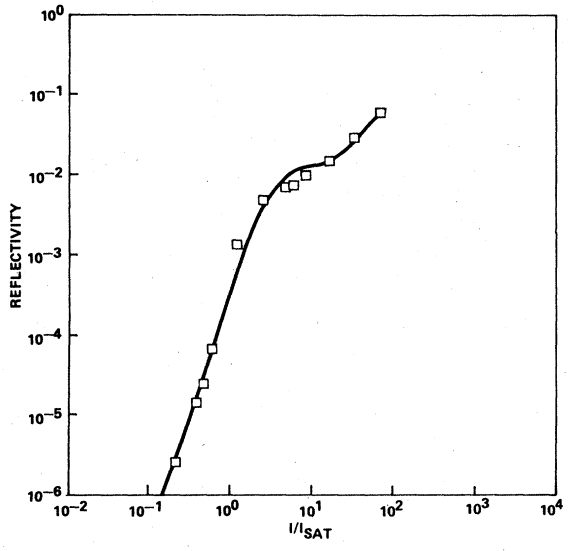

FIG. 9. Comparison of four-level theoretical model with pump absorption to experimental reflectivity measurements ($\tau_p = 1.2$ nsec). The only adjustable parameter is I_{34}^s/I_{12}^s.

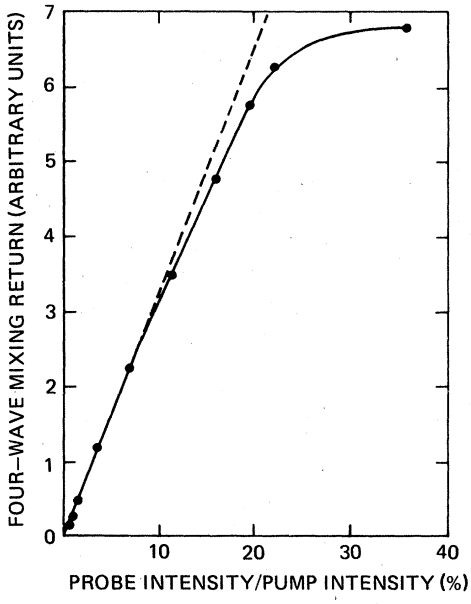

FIG. 10. DFWM return as a function of the probe-to-pump intensity ratio. The region of validity of the small signal regime is in the linear portion of this curve. The saturation of the return is because of saturation in the absorption caused by the probe.

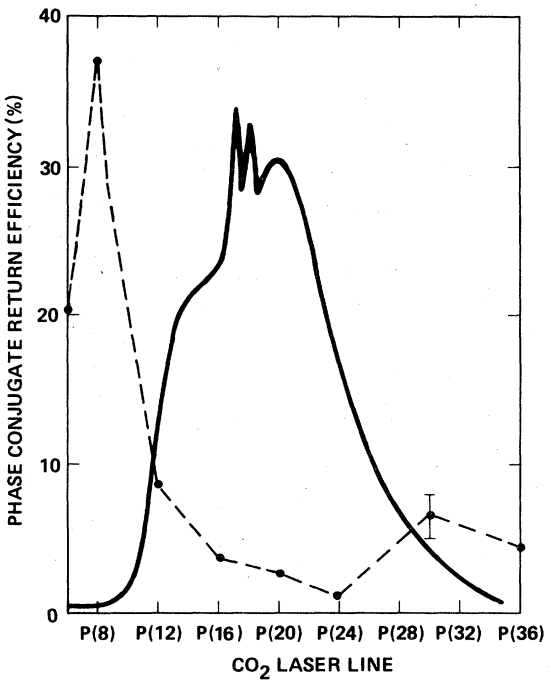

FIG. 11. DFWM reflectivity as a function of wavelength in SF_6. The dotted line represents the experimental measurements of DFWM. For each measurement the pressure was optimized. The solid line represents the absorption in SF_6 (arbitrary units). The largest reflectivities were obtained in the P(8) line at 60 Torr in the region where the interaction is primarily because of the nonlinear dispersion rather than the nonlinear absorption.

band, the response is dominated by pure absorption. The anomalous dispersion contribution to the nonlinearity is negligible since contributions on one side of the resonance are opposite in sign to those from the opposite side (as discussed above). However, at the higher and lower frequencies, the absorption is falling off quite rapidly, leaving a primarily dispersive response. This results in a reflectivity of 38% at the P(8) line; much higher than predicted by theory for zero detuning (i.e., $\delta = 0$). Such a dependence clearly supports the expected off-resonant behavior.

The pressure dependence of the DFWM reflectivity for a simple two-level homogeneously pressure-broadened system can be obtained from the homogeneous theory discussed above if one takes the appropriate pressure dependences. In particular, one must adjust T_1 and T_2 (the longitudinal and transverse relaxation times) and hence the normalized detuning parameter, δ, and the saturation intensity, I_{sat}. However, the problem for SF_6 is greatly complicated by the contribution of pressure-broadened lines far off line center. A calculation proved too difficult but Fig. 12 shows

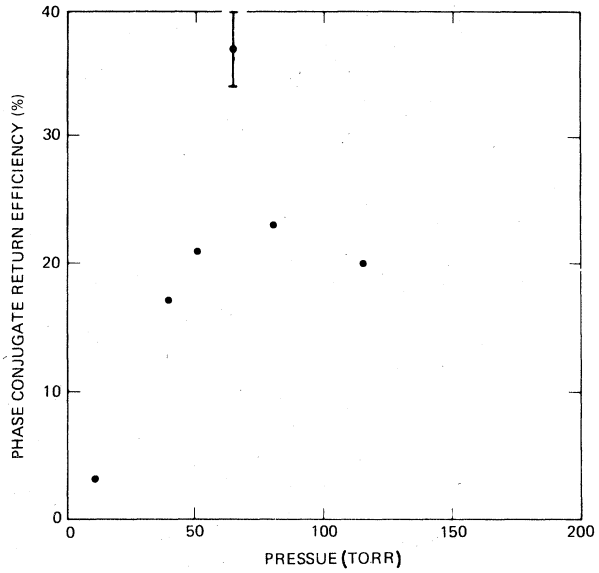

FIG. 12. Pressure dependence of DFWM reflectivity on the P(8) line of CO_2 in SF_6.

the observed pressure dependence on the P(8) line reflectivity.

Correction of an aberrated probe beam was demonstrated in both the long-and short-pulse regime. The aberration was provided by inserting a salt flat whose surfaces were aberrated by etching in water. The aberration was inserted in the path of the probe beam just before the beam entered the cell. The signal was observed in the far field of a 30-in focal-length lens on the infrared vidicon. Details of these measurements and the excellent aberration correction is given in Ref. 18.

The results discussed thus far pertain to nonlinear processes arising from the first two terms in Eq. (3); the incoherent absorption-dispersion terms. At the power levels for the above long-pulse data, we experimentally observed no contribution from the third term in Eq. (4) when the probe-beam polarization was rotated $\pi/2$ rad, thus eliminating the first two terms. While the physical origin of the susceptibility describing this third term (the coherent term) depends on the system involved, for SF_6 at 10 Torr, we believe the important description is based on the two-photon (TP) interaction discussed above. In particular, $\vec{E}_f \cdot \vec{E}_b$ oscillates at $2\omega_0$ of the laser frequency. As we discussed,[4] this effect becomes important in the limit that the TP Rabi frequency is comparable to the TP dephasing rate, i.e.,

$$\omega_R^{TP} \gtrsim (T_2^{TP})^{-1}.$$

The experimental study proceeded using 1-nsec pulses on various CO_2 lines of the 10.4-μm branch.

The DFWM configuration was the same as discussed above. The pump intensities were of order 5 MW/cm^2, and the interaction region was 10 cm. The cell could be cooled to 140°K, where the reflectivities were observed to be highest. Shown in Fig. 13 is a plot of the measured reflectivity as a function of wavelength at 140°K. The reflectivity is highest at the P(16) line. In fact, the TP signal equals the one-photon contribution. Owing to the discrete tuning nature of CO_2 lasers, we were unable to precisely locate the TP resonance frequency. However, the approximate location is consistent with computer simulations of SF_6 (Ref. 32). The signal return observed at the P(16) line was measured at both 140° and 300°K showing a factor of 10 increase at 140°K. As we have noted this is expected if the transition arises from ground-state populations. The ground-state population at the P(16) line increases by three at 140°K. Since the signal varies as the number density squared, we can conclude that a ground-state transition and not hot-band transitions is responsible for this resonance.

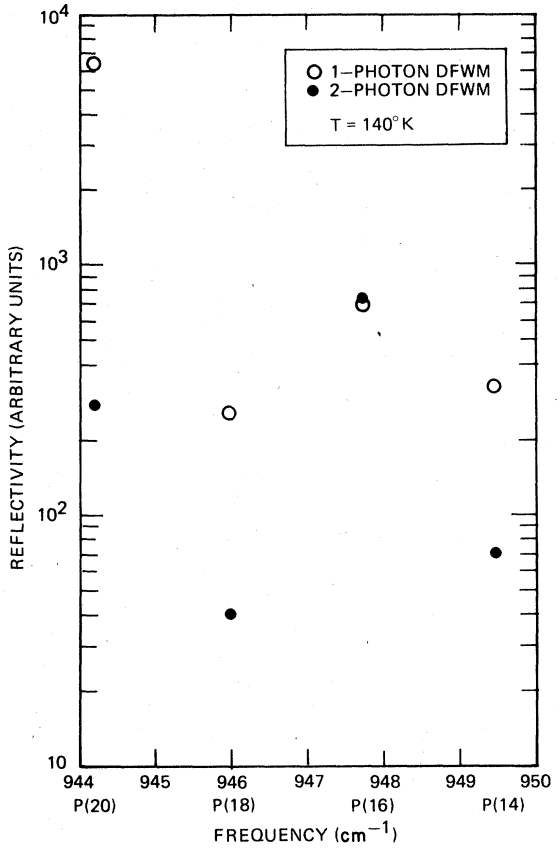

FIG. 13. A comparison of reflectivity for one-photon DFWM and two-photon DFWM measured in SF_6 at 140 K and 1-Torr pressure in a 10-cm long cell. Note that on the P(16) line the 1 and 2 photon contributions are equal.

The room temperature pressure dependence is shown in Fig. 14. The decrease in signal at high pressure is due to absorption.

The TP contribution to DFWM has some interesting properties. First, due to the counterpropagating pumps, the signal is Doppler free. This has obvious useful spectroscopic implications (see Refs. 3 and 4). Also, since no grating results from spatial hole burning, there is no motional washout to degrade the signal. Finally, since in general the intermediate state is detuned from resonance, there is no radiative state involved in this interaction. This implies the potential for a greatly improved signal-to-noise ratio in the reflectivity.

An alternative explanation of this coherent term is Zeeman coherence[2] between degenerate magnetic substrates briefly mentioned above. We have observed this in our CW DFWM experiments at 50 mTorr in SF_6 discussed elsewhere.[21] However, it is anticipated that such effects are eliminated by dephasing collisions at high pressure and would not have the spectral structure of Ref. 4.

For some applications, it may be necessary to consider DFWM of multiwavelength radiation. The DFWM theory for broadband materials is

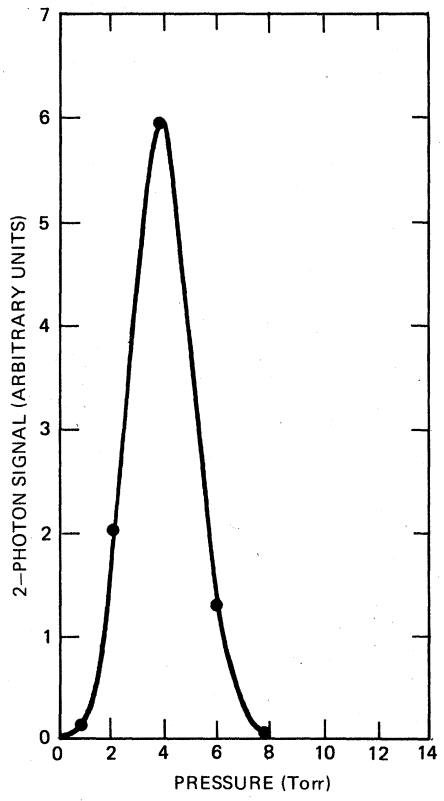

FIG. 14. Measurement of the two-photon signal as a function of pressure ($T = 300$ K).

significantly different than for resonant materials. Three-level resonant theory shows the potential for very interesting, novel spectroscopy. We have experimentally observed simultaneous DFWM in addition to multiwavelength phase conjugation for adjacent CO_2 lines in SF_6 and have discussed this elsewhere.[33]

CONCLUSION

Our experiments have demonstrated many important aspects of DFWM. Despite the complex spectroscopy of SF_6, we have demonstrated agreement between a four-level theory and experiment in a homogeneously broadened system. In addition, we have observed two-photon DFWM and shown that it can equal one-photon processes on resonance. The importance of DFWM is recognized both for its spectroscopic power and phase conjugation properties. The intrinsic simplicity of this technique coupled with its high signal-to-noise ratio and a detailed theoretical understanding make it a very powerful tool in both of the above applications.

ACKNOWLEDGMENTS

The authors would like to thank C. R. Giuliano and R. L. Abrams for valuable technical discussions and suggestions, and J. Schuler for valuable technical assistance in fabrication of much of the facility. The work was supported in part by Department of Energy Contract No. DE-AC08-78DP 40023 and Los Alamos Scientific Laboratory Contract No. 4-L90-7269M-1.

[1]P. F. Liao, D. M. Bloom, and N. P. Economou, Appl. Phys. Lett. 32, 813 (1978).
[2]J. F. Lam, D. G. Steel, R. A. McFarlane, and R. C. Lind, Appl. Phys. Lett. (in press).
[3]P. F. Liao, N. P. Economou, and R. R. Freeman, Phys. Rev. Lett. 39, 1473 (1977).
[4]D. G. Steel and J. F. Lam, Phys. Rev. Lett. 43, 1588 (1979).
[5]S. M. Wandzura, Opt. Lett. 4, 208 (1979).
[6]J. F. Lam (unpublished).
[7]Tao-Yi Fu and Murray Sargent III, Opt. Lett. 5, 433 (1980).
[8]R. K. Raj, D. Bloch, J. J. Snyder, G. Camy, and M. Ducloy, Phys. Rev. Lett. 44, 1251 (1980).
[9]B. I. Stepanov, E. V. Ivakin, A. S. Rubanov, (Dok. Akad. Nauk. SSSR 196, 567 (1971) [Sov. Phys. Dokl. 16, 46 (1971)].
[10]A. Yariv, IEEE J. Quantum Electron. QE-14, 650 (1978).
[11]David M. Pepper, Dan Fekete, and Amnon Yariv, Appl. Phys. Lett. 33, 41 (1978).
[12]R. K. Jain and M. B. Klein, Appl. Phys. Lett. 35, 454 (1979); R. K. Jain, M. B. Klein, and R. C. Lind, Opt. Lett. 4, 328 (1979).
[13]R. L. Abrams and R. C. Lind, Opt. Lett. 2, 94 (1978); 3, 235 (E) (1978).
[14]D. Grischkowsky, N. S. Shiren, and R. J. Bennett, Appl. Phys. Lett. 33, 805 (1978).
[15]D. M. Bloom, P. F. Liao, and N. P. Economou, Opt. Lett. 2, 58 (1978).
[16]P. F. Liao and D. M. Bloom, Opt. Lett. 3, 0 (1978).
[17]Robert A. Fisher and B. J. Feldman, Opt. Lett. 4, 140 (1979).
[18]R. C. Lind, D. G. Steel, M. B. Klein, R. L. Abrams, C. R. Giuliano, and R. K. Jain, Appl. Phys. Lett. 34, 457 (1979).
[19]Henri Brunet, IEEE J. Quantum Electron. QE-6, 678 (1970).
[20]D. G. Steel, R. C. Lind, J. F. Lam, and C. R. Giuliano, Appl. Phys. Lett. 376, 35 (1979).
[21]D. G. Steel and J. F. Lam (unpublished).
[22]A. Yariv and D. M. Pepper, Opt. Lett. 1, 16 (1977).
[23]B. K. Garside, R. S. Taylor, and E. A. Ballik, Can. J. Phys. 55, 849 (1977).
[24]John J. Armstrong and Oscar L. Gaddy, IEEE J. Quantum Electron. QE-8, 797 (1972).
[25]J. F. Lam and G. J. Dunning (unpublished).
[26]G. J. Dunning and D. G. Steel, IEEE J. Quant. Electron. (in press).
[27]J. T. Knudtson and G. W. Flynn, J. Chem. Phys. 58, 1467 (1973).
[28]V. N. Bagratashvili, V. S. Dolzhikov, and V. S. Letokhov, Zh. Eksp. Teor. Fiz. 76, 18 (1979) [Sov. Phys.—JETP 49, 8 (1979)].
[29]S. Czuchlewski, A. V. Nowak, and E. Foley, Proceedings of the Electro-Optics/Laser '77 Conference October 1977, Anaheim, CA., pp. 303-311 (LASL Report LA-UR 77-2251) (unpublished).
[30]W. P. Brown (unpublished).
[31]R. S. McDowell, H. W. Galbraith, B. J. Krohn, C. D. Cantrell, and E. D. Hinkley, Opt. Commun. 17, 183 (1976).
[32]J. R. Ackerhalt and H. W. Galbraith, J. Chem. Phys. 69, 1200 (1978).
[33]Duncan G. Steel and Juan F. Lam, Opt. Lett. 5, 297 (1980).